

# Quasi-ballistic Transport in Submicron $\text{Hg}_{0.8}\text{Cd}_{0.2}\text{Te}$ Diodes: Hydrodynamic Modeling

M. Daoudi, A. Belghachi and L. Varani

**Abstract**—In this paper, we analyze the problem of quasi-ballistic electron transport in ultra small of mercury -cadmium-telluride ( $\text{Hg}_{0.8}\text{Cd}_{0.2}\text{Te}$  -MCT)  $n^+n^-n^+$  devices from hydrodynamic point view. From our study, we note that, when the size of the active layer is low than  $0.1\mu\text{m}$  and for low bias application ( $\geq 9\text{mV}$ ), the quasi-ballistic transport has an important effect.

**Keywords**— $\text{Hg}_{0.8}\text{Cd}_{0.2}\text{Te}$  semiconductor, Hydrodynamic mode, Quasi-ballistic transport, Submicron diode

## I. INTRODUCTION

RECENT advances in technology leads to increasing high speed performance of submicron electron devices by the scaling of both process and geometry. In order to aid the design of these devices, it is necessary to use powerful numerical simulation tools [1-3]. It is necessary to use more refined models, including higher order moment of the distribution function, in order to correctly predict the behavior of device [4, 5]. Several models have been considered as viable simulation tools, among these models we have hydrodynamic model (HD). The full hydrodynamic model consists of the continuity equations expressing the conservation of mass, momentum, and energy taking three moments of the Boltzmann transport equation with suitable approximations [6]. In our previous work [7], we have demonstrated the robustness of the hydrodynamic model to simulate the electronic transport in the bulk of  $\text{Hg}_{0.8}\text{Cd}_{0.2}\text{Te}$  (MCT) semiconductor at 77K, where majority MCT semiconductors based devices contain a cadmium fraction  $x = 0.2$  which allows, at 77 K, detection in the 8–14  $\mu\text{m}$  spectral region, which is a widely used alloy for infrared optoelectronics applications [8]. In this paper, we are interested to simulate the quasi-ballistic transport for one-dimensional  $\text{Hg}_{0.8}\text{Cd}_{0.2}\text{Te}$   $n^+n^-n^+$  structure modeling by the HD model coupled with the Poisson equation in high electric field.

## II. THEORETICAL MODEL

The hydrodynamic model consists of a set of equations expressing the conservation of charge, momentum and energy for each species of carriers. These equations are derived by taking the first three moments of the Boltzmann transport equation [9-12]. For one dimension of the electron component (neglecting electron-hole generation and recombination with is inessential for the applications we shall present in the sequel paper), these equations comprise: The particle number balance equation;

M. DAOUDI Laboratoire physique et dispositifs à semiconducteurs, Université de Béchar, n°417, Béchar (08000), Algérie. (Phone : 213664432795, Fax :-21349819155, E-mail : daoudimadz@yahoo.fr)

A. BELGHACHI Laboratoire physique et dispositifs à semiconducteurs, Université de Béchar, n°417, Béchar (08000), Algérie. (E-mail : abelghachi@yahoo.fr).

L. VARANI Institut d'Electronique du sud, UMR CNRS 5214, Université Montpellier II, c.c.084, place Bataillon, 34095 Montpellier Cedex 5, France. (E-mail : Luca.VARANI@univ-montp2.fr)

$$\frac{\partial n}{\partial t} + \frac{\partial(n.v)}{\partial x} = 0, \quad (1)$$

The velocity balance equation;

$$\frac{\partial v}{\partial t} + v. \frac{\partial v}{\partial x} + \frac{1}{n}. \frac{\partial(n.Q_v)}{\partial x} + \frac{q.E}{m^*} = -\frac{v}{\tau_v}, \quad (2)$$

The energy balance equation.

$$\frac{\partial \varepsilon}{\partial t} + v. \frac{\partial \varepsilon}{\partial x} + \frac{1}{n}. \frac{\partial(n.Q_\varepsilon)}{\partial x} + q.E.v = -\frac{\varepsilon - \varepsilon_0}{\tau_\varepsilon}. \quad (3)$$

Where

$$Q_v \equiv \langle \delta v^2 \rangle = \langle v^2 \rangle - \langle v \rangle^2 \quad (4)$$

$$Q_\varepsilon \equiv \langle \delta v \delta \varepsilon \rangle = \langle v. \varepsilon \rangle - \langle v \rangle. \langle \varepsilon \rangle \quad (5)$$

For the modeling of voltage driven operation, where a constant voltage is applied between the structure terminals, Eq. (1), Eq.(2) and Eq.(3) are coupled with the Poisson equation given by:

$$\frac{\partial E}{\partial x} = \frac{q}{\varepsilon_{sc}}(n - Nd); \quad (6)$$

Here  $m^*$  is the electron effective mass,  $n$ ,  $v$ ,  $\varepsilon$  are the electron density, average velocity and mean energy,  $E$  is the electric field,  $q$  is the absolute value of the electric charge.  $Nd$  is the ionized donor density and  $\varepsilon_{sc}$  is the lattice dielectric constant. Finally,  $\tau_v$  and  $\tau_\varepsilon$  are the velocity and energy relaxation time,  $Q_v$  and  $Q_\varepsilon$  the velocity variance and velocity-energy covariance respectively. This system of equations contains four unknowns which are the electron density, the average velocity, mean energy and electric field. Moreover, it contains five input parameters: the effective mass, the velocity, energy relaxation times, the velocity variance and velocity-energy covariance respectively. We note that the parameters of this system of equations are, by definition, functions of the mean energy [13-14]. These coefficients are not fitting parameters but rather will be extracted by Monte Carlo data obtained by C. Palermo code [15]. Following standard procedures, these differential equations are turned into difference equations on space- time grid. A generalized central difference finite scheme for the hydrodynamic equation coupled with Poisson equation has been employed on the numerical algorithm. This discretization scheme has shown global convergence in our program; which are extremely stable

and robust, especially suitable for strong convective regimes, for more detail see ref. [16-19].

### III. SIMULATION RESULTS

The consider  $\text{Hg}_{0.8}\text{Cd}_{0.2}\text{Te}$   $n^+-n-n^+$  diode in which the low-doped diode base  $n$  of length  $L$  is sandwiched between two heavily doped contacts  $n^+$ . The parameters of this simulated structure are; the  $n^+$  regions are each  $0.2\mu\text{m}$  thick with a doping density of  $5.410^{15}\text{ cm}^{-3}$ , the  $n$  central region is  $0.2\mu\text{m}$  of thickness and a doping density of  $10^{14}\text{ cm}^{-3}$ . Initially the electrons are in thermal equilibrium with the lattice at  $T=77\text{K}$ . The carriers' densities are assumed equal to the doping densities (fully ionized impurities). This device is quite simple but suitable for understanding the aim features of non-equilibrium transport and the effect of carrier energy or temperature. In our simulation, we have the left terminal of the diode ground (zero bias), and a positive bias is applied to the right terminal, so that the electrons are injected from the left end and move toward the right end. We assume that the contacts are ideal ohmic contacts. From this assumption, it preserves charge neutrality and thermal equilibrium at the contacts. The results of simulations of various quantities obtained for the different symmetrical structures are showing in figure 1. Three different applied voltages are considered  $0.003\text{V}$ ,  $0.009$  and  $0.015\text{V}$ , present the ohmic and the sutured regimes respectively. In the calculation, we carried out several simulations on this structure and we present for each case, the concentration, the mean velocity, the energy and electric field are plotted versus position respectively in fig. 1. From fig. 1, we see that an important electron injection in the central region due to diffusion from  $n^+$  regions -the carrier density is various from  $10^{14}$  to  $5 \times 10^{14}\text{ cm}^{-3}$  - in conjunction with the quasi-linear variation of the electric field fig. 1(a) and fig. 1(d); when the voltage is applied to the structure, the potential barrier begging to decrease in the first  $n^+/n$  homo-junction as the voltage bias increase, and the potential mostly drops inside the  $n$  region. As a consequence of the fall in the voltage barrier, the positive value of electric field in the first  $n^+/n$  homo-junction decreases, and a very high negative electric field is found in the active layer ( $n$  region), which reaches a maximum in second  $n/n^+$  homo-junction, it is about  $-1.5\text{ KV/cm}$ . Furthermore, in the  $n$  region the main contribution comes from the electric field term, where a significant number of high- energy electrons penetrate in the active layer fig. 1(b).

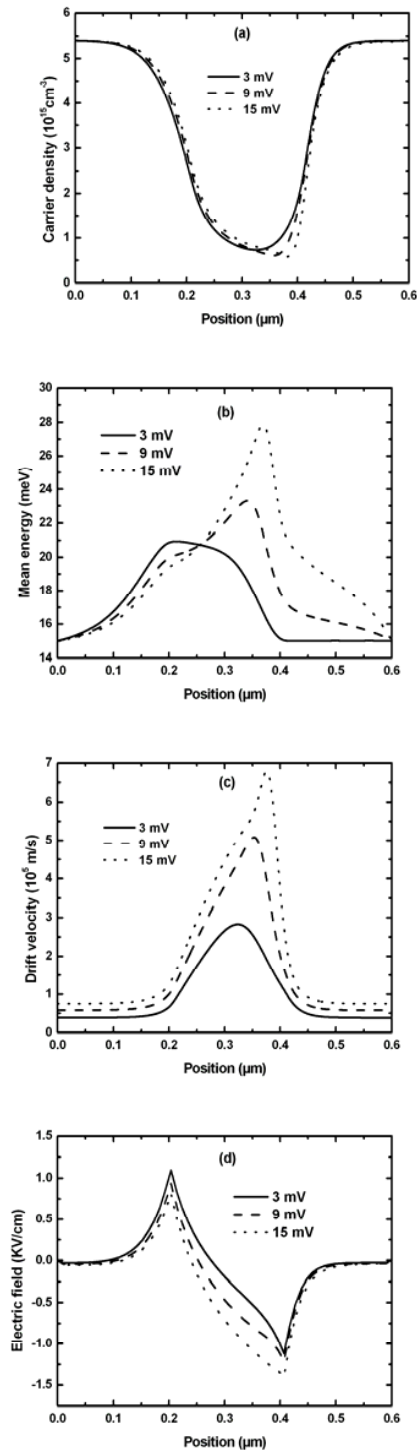


Fig. 1 Stationary profiles for: (a) electron density, (b) mean energy, (c) drift velocity, (d) electric field for  $\text{Hg}_{0.8}\text{Cd}_{0.2}\text{Te}$   $n^+-n-n^+$  diode of length  $0.6\mu\text{m}$  for different applied voltages at  $77\text{K}$ .

Therefore, the average electron velocity exhibit some overshoot at the high field region around  $0.4\mu\text{m}$ , before it reaches the collector fig. 1(c). This effect can be understood in

view of the disparity of the relaxation time for momentum and energy. Indeed, in the  $Hg_{0.8}Cd_{0.2}Te$  semiconductor the energy relaxation time is shorter than the momentum relaxation time [7, 15]. The maximum value of drift velocity as the applied bias increases, it about  $v_{max} = 7 \times 10^5 m/s$ .

In fig. 2, we have studied how the spatial profiles are changed when the active layer (n region) length is scald down from  $0.2\mu m$  to  $0.1\mu m$ , while the length of the structure is fixed in  $0.6\mu m$ . The doping profile of each structure is identical to that of structures already presented with voltage applied to the terminal of the diode equal to  $0.09 V$ .

We see a fort injection of carriers much greater than the active layer is small fig. 2 (a); it is higher than obtained in the first case. This affects the electric field as shown in fig. 2 (d). Indeed, the electric field increases in contacts and its maximum value decreases in the central region from  $1KV/cm$  to  $0.6KV/cm$ , where the size of this region is reduced in half. We can conclude that the device long is enough for the electrons to reach thermal equilibrium for the high- voltage bias, fig. 2(b). It is clearly seen from fig. 2(c), why the hot-electron effects are not pronounced in sub-micrometer diodes. For the semiconductor  $Hg_{0.8}Cd_{0.2}Te$ , this effect is not pronounced when the length of active layer is lower than  $0.1\mu m$ , where the affect of *quasi-ballistic transport* is important.

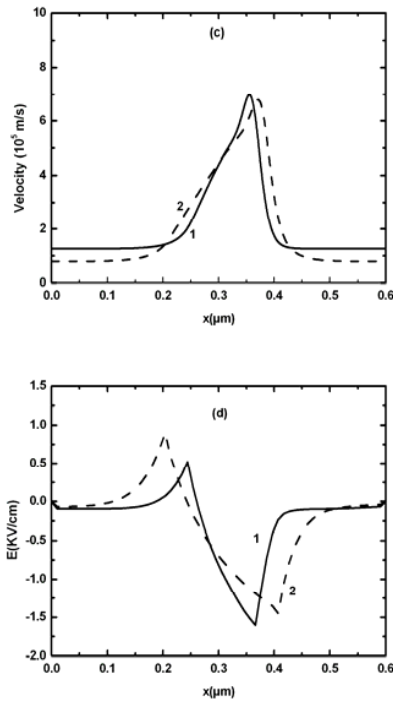


Fig. 2 Stationary profiles for: (a) electron density, (b) mean energy, (c) drift velocity, (d) electric field for  $Hg_{0.8}Cd_{0.2}Te$   $n^+-n-n^+$  diode with different active layer lengths-  $0.1\mu m$  (1) and  $0.2\mu m$  (2), for the same applied bias  $0.09V$  at  $77K$ .

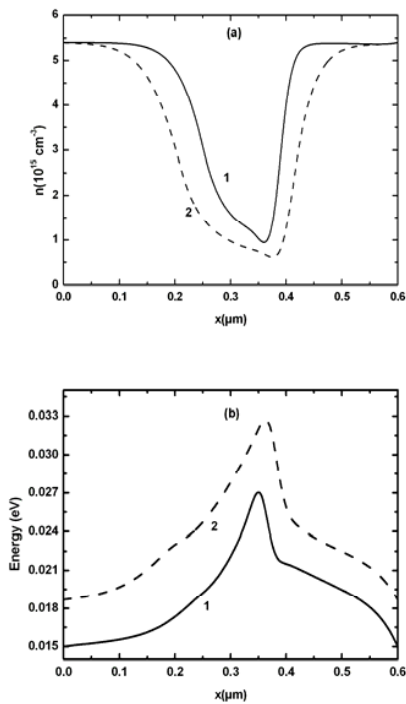


Fig. 3 Currant- voltage characteristic of  $Hg_{0.8}Cd_{0.2}Te$   $n^+-n-n^+$  diode at  $77K$ , for different length of device.

In fig. 3, at low biases ( $\leq 5mV$ ), the  $I-V$  curves are liner for any length, where at high applied biases the characteristics become sub-linear and a current saturation region is more appears; it is due to the saturate phenomenon of drift velocity. This effect is pronounced for long diodes ( $1\mu m$ ), whereas for submicron diodes ( $0.4\mu m$  and  $0.6\mu m$ ) the deviation from the linear dependence is not large in the range of voltages investigated; where the *quasi-ballistic transport* is important for these sort diodes.

## IV. CONCLUSION

Device modeling is playing a very important role in the development of semiconductor device design. In this work, a semiconductor device simulator based on the hydrodynamic balance equation has been developed. We have applied this model to  $\text{Hg}_{0.8}\text{Cd}_{0.2}\text{Te}$   $n^+-n-n^+$  submicron diode. The numerical results demonstrate the basic hot carrier effect involving the spatial velocity overshoot. We also note that the spurious overshoot peak, when electric field drastically increases, does show in our result. The size of the active layer has important role for overshoot behavior and ballistic transport effects.

## REFERENCES

- [1] K Blotekjaer, *IEEE Trans. Electron Devices* **17**, 38 (1970).
- [2] M Trovato, P Falsaperla, *Phys. Rev. B* **57** (8), (1998) 4456 - 4471.
- [3] C. Jacoboni and L. Reggiani, *Rev. Mod. Phys.* **55**, 645-705 (1983).
- [4] V Gruzinskist, E Starikov, P Shiktorov, L reggiani, M Saraniti, L Varani, *Semicond. Sci. Technol.* **8**(1993) 1283- 1290.
- [5] C. Jacobini and P. Lugli, *Springer Verlag*, Vienna (1989).
- [6] E Starikov, P Shiktorov, V Gruzhinskis, T Gonzalez, M J Martin, D Pardo, L Reggiani, L Varani, *Semicond. Sci. Technol.* **11** (1996) 865-872.
- [7] M Daoudi, A Belghachi, L Varani, and C Palermo, *Eur. Phys. J. B* **62**, 15–18 (2008).
- [8] B Gelmont, B Lund, K Kim, G U Jensen, M Shur, T A Fjeldly, *J. Appl. Phys.* **71**, 4977 (1992).
- [9] R C Chen, J L Liu, *J. Comp. Phys.* **189** (2003) 579–606.
- [10] P Degond, S Gallego, F Méhats, *J. Comp. Phys.* **221** (2007) 226–249.
- [11] V K Khanna, *Physics Reports* **398** (2004) 67–131.
- [12] C H Kao, L W Chen, *Solid-State Electronics* **46** (2002) 915–923.
- [13] C M Snowden, Introduction to semiconductor device modelling (World Scientific, 1986)
- [14] L Reggiani, Hot-Electron Transport in Semiconductors, Topics in Applied Physics (Springer-Verlag, Berlin, Heidelberg, 1985), Vol. 58
- [15] C Palermo, L Varani, JC Vaissière, E Starikov, P Shiktorov, V Gruzhinskis, B Azais, *Solid State Electron.* **53**, 70 (2009) 1316-1323.
- [16] A Jünger, S Tang, *Appl. Numer. Math.* **56** (2006) 899–915.
- [17] L V Ballestra, R Sacco, *J. Comp. Phys.* **195** (2004) 320–340.
- [18] A Aste, R Vahldieck, *Int. J. Numer. Model.* **16** (2003) 161–174.
- [19] N R Aluru, K H Law, A Raefsky, P M Pinsky, RW Dutton, *Comput. Methods Appl. Mech. Engrg.* **125** (1995) 187-220.